

42. D'Abaco, G. M., and Kaye, A. H. (2007) Integrins: Molecular determinants of glioma invasion. *Journal of Clinical Neuroscience* **14**, 1041-1048
43. Gladson, C. L., and Cheresch, D. A. (1991) Glioblastoma expression of vitronectin and the alpha v beta 3 integrin. Adhesion mechanism for transformed glial cells. *The Journal of Clinical Investigation* **88**, 1924-1932
44. Wadehra, M., Iyer, R., Goodglick, L., and Braun, J. (2002) The tetraspan protein epithelial membrane protein-2 interacts with beta1 integrins and regulates adhesion. *J Biol Chem* **277**, 41094-41100
45. Loriger, M., and Felding-Habermann, B. (2012) Integrin Signaling in Angiogenesis and Metastatic Cancer Progression in the Brain Signaling Pathways and Molecular Mediators in Metastasis. (Fatatis, A. ed.), Springer Netherlands. pp 311-329
46. Kawaguchi, T., Yamashita, Y., Kanamori, M., Endersby, R., Bankiewicz, K. S., Baker, S. J., Bergers, G., and Pieper, R. O. (2006) The PTEN/Akt pathway dictates the direct alphaVbeta3-dependent growth-inhibitory action of an active fragment of tumstatin in glioma cells in vitro and in vivo. *Cancer Res.* **66**, 11331-11340
47. Chang, M.-W., Lo, J.-M., Juan, H.-F., Chang, H.-Y., and Chuang, C.-Y. (2012) Combination of RGD Compound and Low-Dose Paclitaxel Induces Apoptosis in Human Glioblastoma Cells. *PLoS One* **7**, e37935
48. Kerbel, R. S. (2008) Tumor Angiogenesis. *New England Journal of Medicine* **358**, 2039-2049
49. Frank, R. T., Aboody, K. S., and Najbauer, J. (2011) Strategies for enhancing antibody delivery to the brain. *Biochimica et Biophysica Acta (BBA) - Reviews on Cancer* **1816**, 191-198
50. McEarchern, J. A., Oflazoglu, E., Francisco, L., McDonagh, C. F., Gordon, K. A., Stone, I., Klussman, K., Turcott, E., van Rooijen, N., Carter, P., Grewal, I. S., Wahl, A. F., and Law, C.-L. (2007) Engineered anti-CD70 antibody with multiple effector functions exhibits in vitro and in vivo antitumor activities. *Blood* **109**, 1185-1192
51. Fukai, J., Nishio, K., Itakura, T., and Koizumi, F. (2008) Antitumor activity of cetuximab against malignant glioma cells overexpressing EGFR deletion mutant variant III. *Cancer Science* **99**, 2062-2069

Table 1. Correlation of EMP2 and pSRC expression in GBM patient samples

N=87	EMP2 positive	EMP2 negative	Total
pSRC positive	49	1	50
pSRC negative	20	17	37

Spearman's rank correlation coefficient,  $r = 0.54$ ,  $p < 0.01$

## FIGURE LEGENDS

**Figure 1. EMP2 expression is increased in GBM.** (A) EMP2 mRNA expression (Affymetrix microarray) was increased in GBM compared to normal brain.  $*p<0.001$ . (B) Survival data for high and low EMP2 mRNA expression. (C) Left, EMP2 expression was increased in GBM tumors compared to normal regions. Right, EMP2 expression was evaluated in a panel of GBM cells lines and in lines derived from patients by western blotting analysis.  $\beta$ -actin expression was used as a loading control. (D-E) GBM tissue arrays containing 329 cores from 110 patients were stained for EMP2 expression. (D) EMP2 protein expression was determined in normal brain, in GBM, and in secretory endometrium (positive control) using an EMP2 polyclonal antibody. To detail nonspecific staining, rabbit preimmune serum was used. Staining was visualized using deNovo Red. Nuclei were counter stained using hematoxylin. (E) EMP2 expression was quantitated on a 0-3 histological scale by two independent pathologists, and the average IHC score shown. (F) EMP2 expression was dichotomized based on high (histological score  $\geq 2$ ) or low (histological score  $\leq 1$ ) expression. High EMP2 expression correlated with a poor survival.

**Figure 2. EMP2 expression promotes GBM tumorigenicity.** (A) U373 modified cell lines were created that overexpress EMP2, express a vector control, or express reduced levels of the protein. U373/EMP2, U373/V, and U373/RIBO cells were then inoculated subcutaneously into athymic nude mice. Tumor volume was calculated twice a week for 50 days.  $N=4$  per group. \*, Comparison of U373/EMP2 with U373/V or U373/V with U373/RIBO by Student's *t* test,  $p<0.05$ . Bottom, EMP2 expression was determined using western blot analysis in U373/EMP2, U373/V, and U373/RIBO cells. Overexpression of EMP2 in these cells is via a GFP-EMP2 fusion protein (48kD). (B) U87/EMP2, U87/V, and U87/shRNA cells were created and injected as above. Tumor volume was monitored for 27 days.  $N=4$  per group. \*,  $p<0.05$  by Student's *t* test. Bottom, Expression of EMP2 in the U87/EMP2, U87/V, and U87/shRNA cells was determined by western blot analysis. In U87MG cells, EMP2 was overexpressed using a bicistronic vector (18kD). (C) EMP2 expression was modified in U373, U87MG, and GM97 cells. In order to reduce EMP2 levels, GM97 were transiently transfected with a control or EMP2 specific siRNAs. In U373 and U87MG cells, EMP2 expression was stably reduced using a ribozyme (RIBO).  $\alpha\beta 3$  integrin surface expression was measured using flow cytometry, and a representative histogram is shown. Right, Values represent the average mean fluorescent intensity (MFI)  $\pm$ SEM from 3 experiments. \*,  $p<0.05$ . N.S., not significant.

**Figure 3. EMP2 promotes GBM invasion.** (A) U373/EMP2, U373/V, or U373/RIBO cells were grown to form a monolayer. A scratch was then created and closure of the wound was measured after 24 hours. Experiments were performed at least three times, and the results were averaged. (B) Equal numbers of U373/EMP2, U373/V, and U373/RIBO were plated into the top of the transwell. After 6 hours, cells that had migrated through the transwell were fixed, stained with crystal violet, and counted. Values are averages of 3 independent experiments ( $\pm$ SEM). (C) U373/EMP2, U373/V, or U373/RIBO cells or (D) T98/EMP2, T98/V, or T98/RIBO cells were added to transwells coated with collagen I or fibronectin. Cells that had invaded through the transwell were determined as above. The experiment was repeated three times, with the data presented as the mean  $\pm$  SEM. (A) through (D): Student's *t* test was used to determine significant differences between groups with specific *p* values indicated in the figure; N.S., not significant. (E) T98/EMP2 or (F) T98/V cells were preincubated with varying concentrations of an anti-

EMP2 IgG1, anti- $\alpha$ v $\beta$ 3 integrin, or isotype control antibody. Cells were then plated onto a fibronectin precoated transwell, and percent invasion relative to the isotype control was determined. Results represent averaged results from 3 independent experiments  $\pm$ SEM. \*,  $p < 0.05$ .

**Figure 4. EMP2 expression promotes activation of FAK and Src.** (A) Panels of U373 or U87MG cells were created to overexpress EMP2 or downregulate its expression through the use of a ribozymes or shRNA vector. Cells were plated, harvested and probed for activated FAK ( $^{576/577}$ pFAK) and Src ( $^{416}$ pSrc). \*  $p < 0.05$ , Comparison by Student's *t* test. (B) Vector control LN229, GM97, and U87 or cells which overexpress EMP2 were plated for 24 hours, then harvested and probed for activated FAK and Src, total FAK, and  $\beta$ -Actin. Top: representative western blots. Bottom: semi-quantitative analysis of activated FAK and Src levels from 3 independent experiments; comparison by Student's *t* test, \*  $p < 0.05$ . (C) U118, U373, and GM5 cells were transfected with an EMP2 siRNA or control siRNA, and cells were incubated for 48 hours, then harvested and probed as above. Top: representative western blots. Bottom: semi-quantitative analysis of pFAK and pSrc after correction for  $\beta$ -actin levels from 3 independent experiments.

**Figure 5. EMP2 expression promotes tumor migration *in vivo*.** (A) U87/EMP2/Luc, U87/V/Luc or U87/shRNA/Luc cells were stereoscopically implanted into the right frontal lobe of athymic nude mice. Tumor load was monitored using bioluminescence imaging; N=6 per group. \*  $p < 0.05$  by one-way ANOVA. (B) Representative bioluminescence images of mice from each group on Day 1 and Day 11. (C) Representative low and high magnification images from two U87/EMP2, U87/V and U87/shRNA tumors. The high magnification image centers on the brain-tumor margin. Magnification: left, 100X; right, 400X.

**Figure 6. EMP2 antibodies reduced cellular viability and tumor load.** (A)  $2 \times 10^5$  GM5, U87MG, U87/EGFR VIII, T98, and U373 cells were incubated for 72 hours with a vehicle control (PBS) or molar equivalents of the anti-EMP2 Db or anti-EMP2 IgG1. Cellular viability was enumerated using trypan blue exclusion. Data represents viability as a percentage of control from three independent experiments. (B) GM5 and T98 cells were treated as above, with cellular viability determined using annexin V and propidium iodide staining. The experiment was repeated 3 times and a representative graph shown. (C) U87/EGFR VIII cells were inoculated subcutaneously in Balb/c nude mice. When tumors reached  $4 \text{ mm}^3$ , they were treated twice weekly (first week, 1.0 mg/kg; second week, 2.5mg/kg), with anti-EMP2 Db or control Db. Left, tumor size (arrow indicates start of treatment). Right, tumor histology after treatment. Magnification, 100X. N=6. \*  $p < 0.05$  as determined by Student's *t* test. (D) U373 cells were subcutaneously injected into athymic nude mice. When tumors reached  $4 \text{ mm}^3$ , mice were treated systemically (i.p.) with anti-EMP2 IgG1 or control IgG (3mg/kg). Left, tumor growth. Right, tumor histology at day 65. Magnification, 100X. N=6. \*  $p < 0.05$  as determined by Student's *t* test.

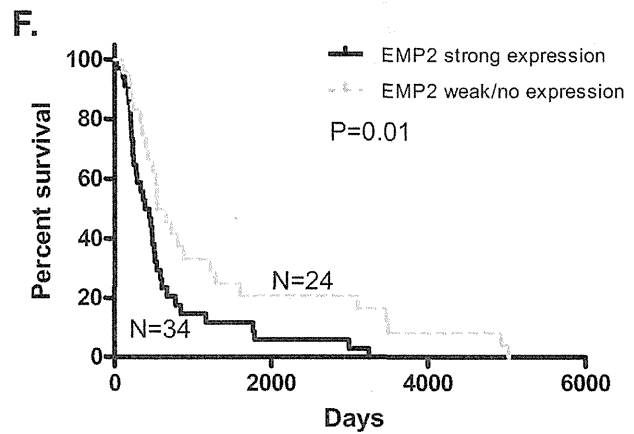
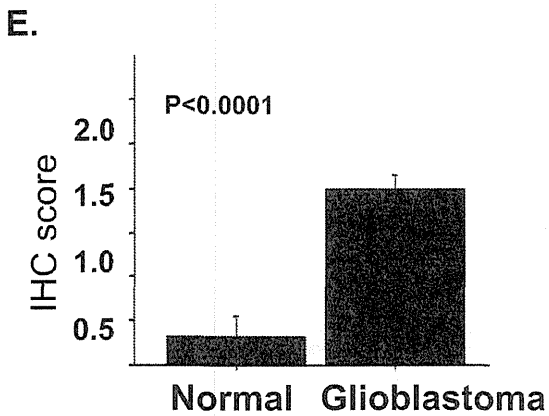
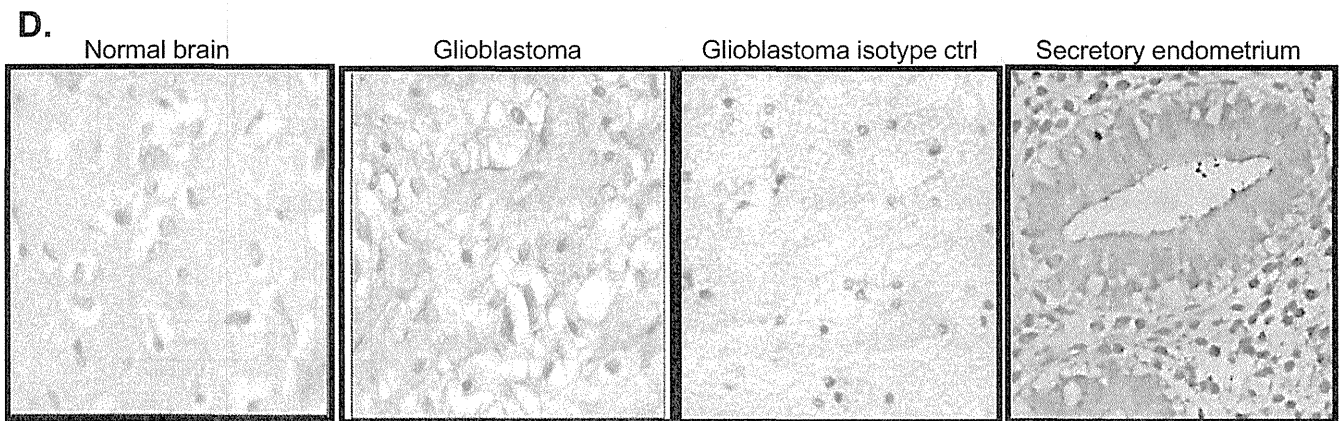
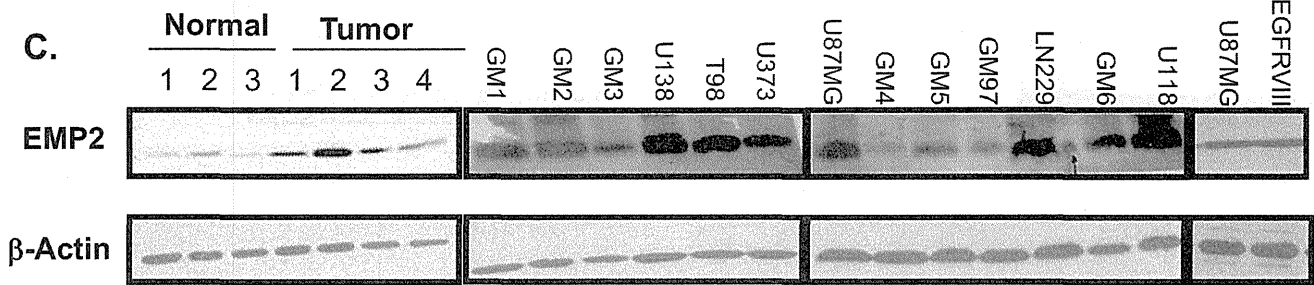
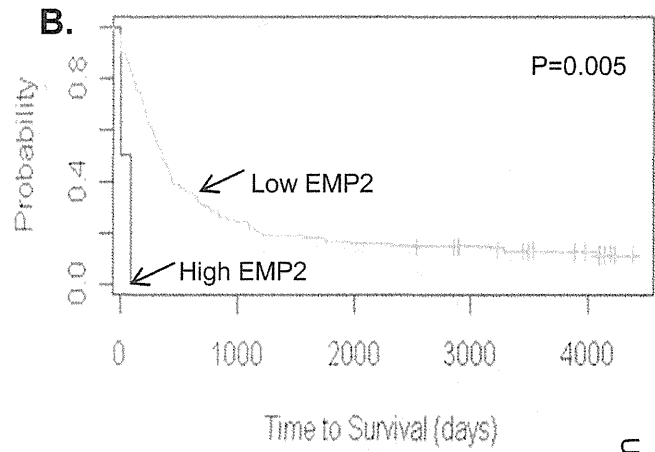
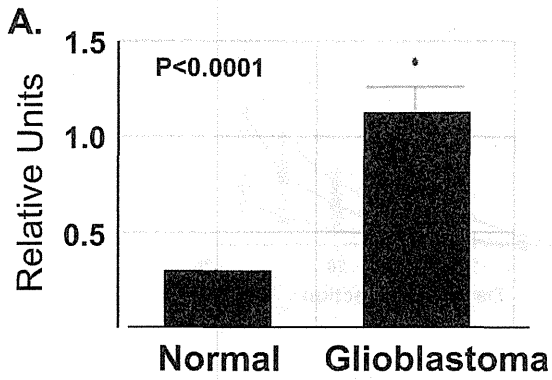
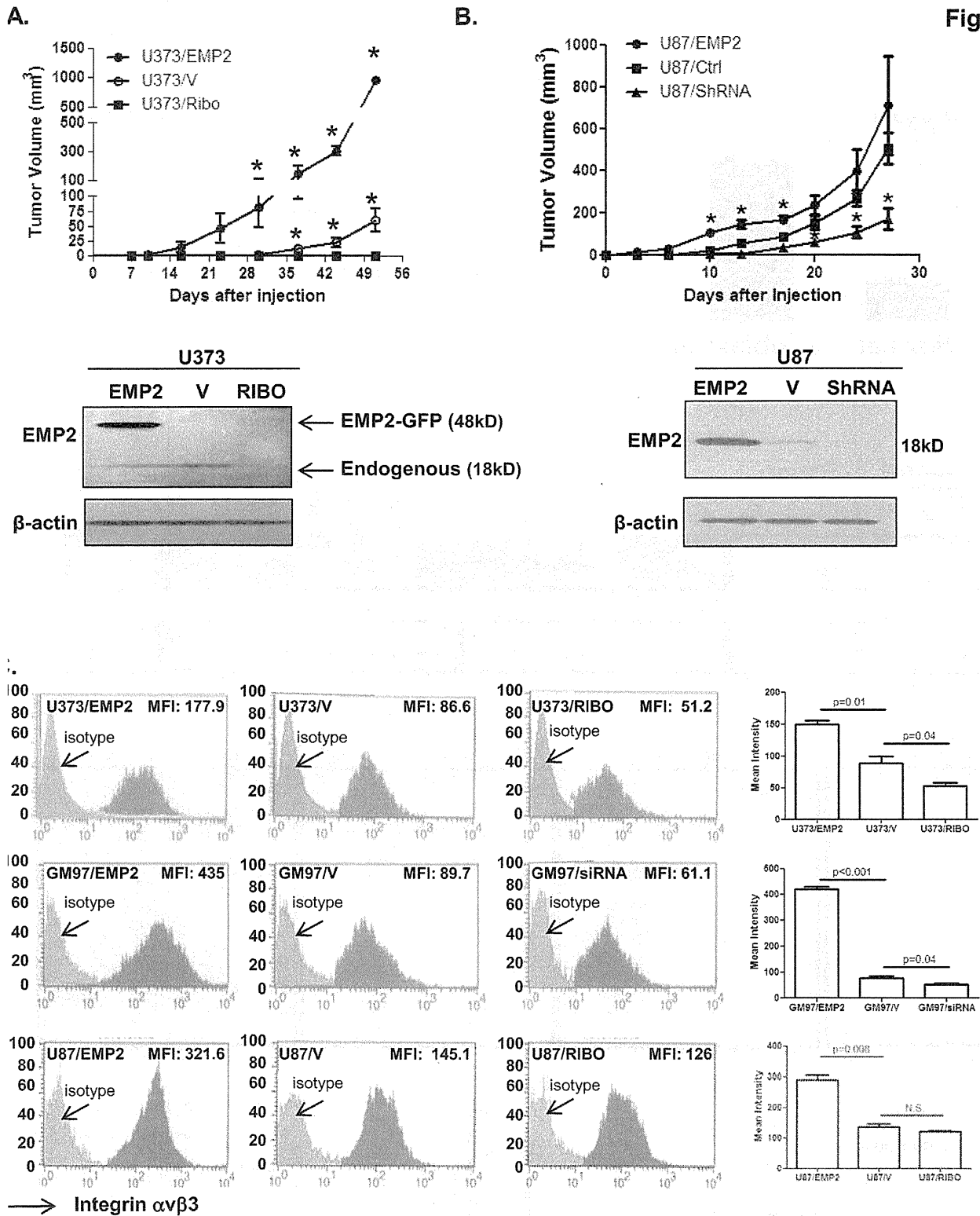
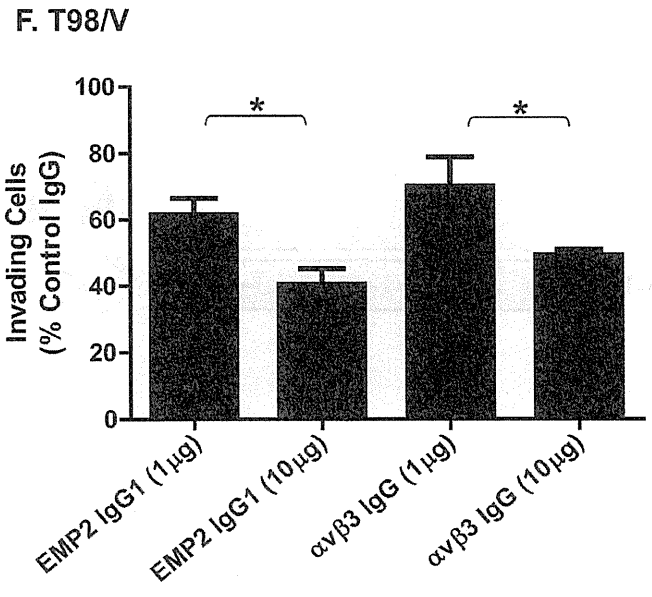
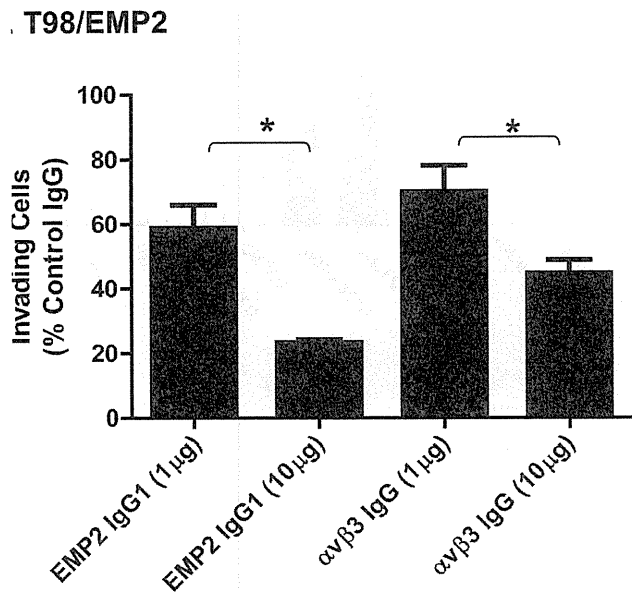
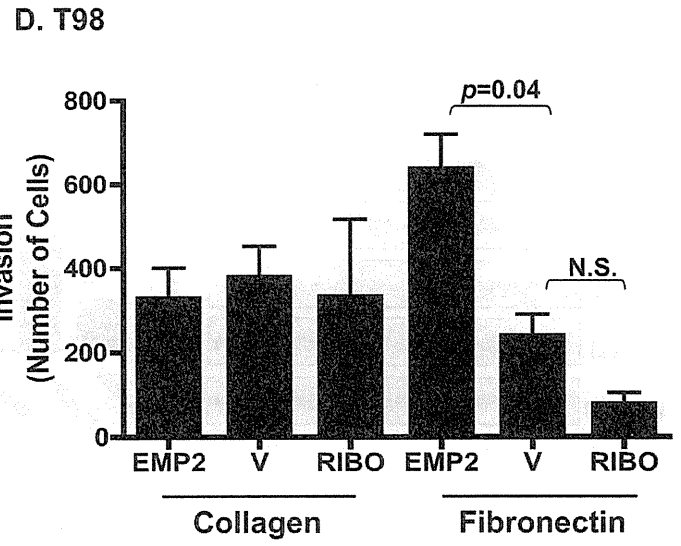
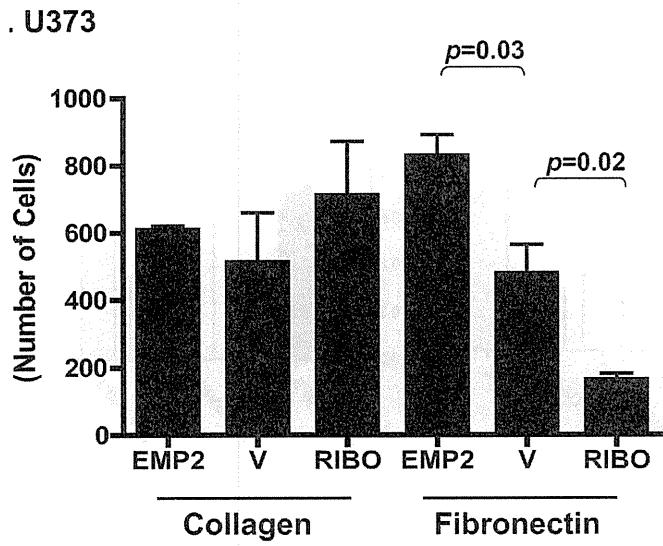
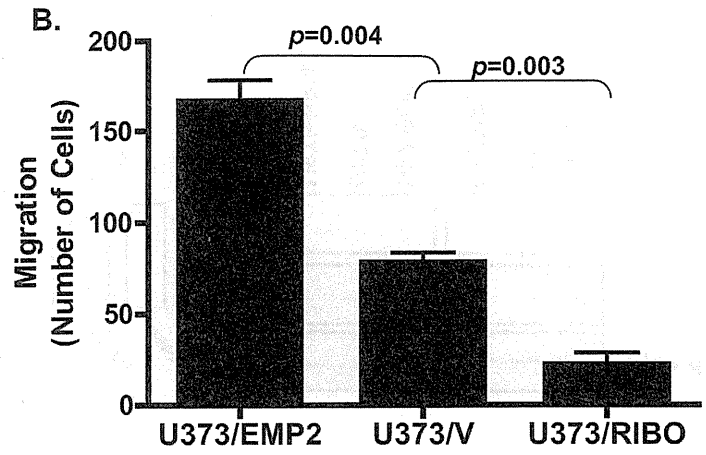
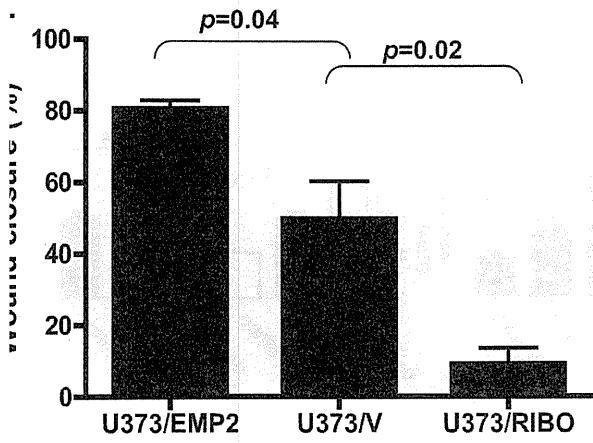
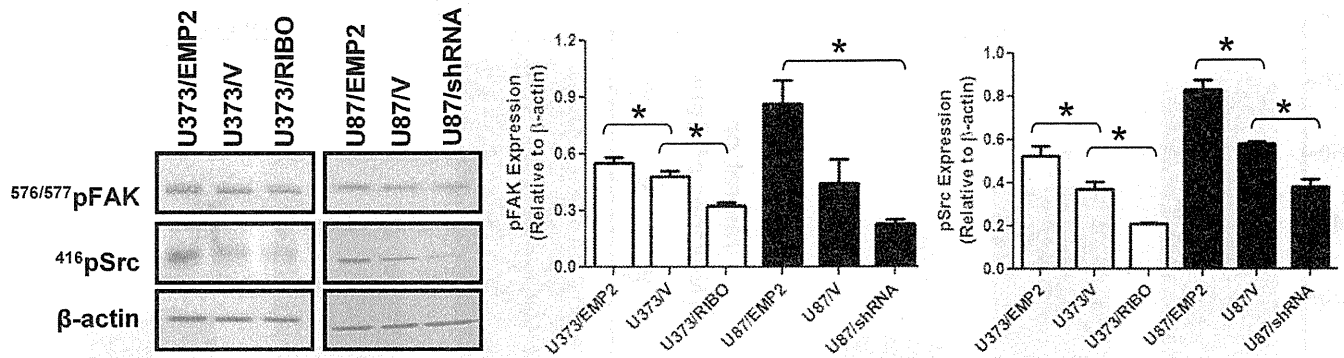


Figure 2

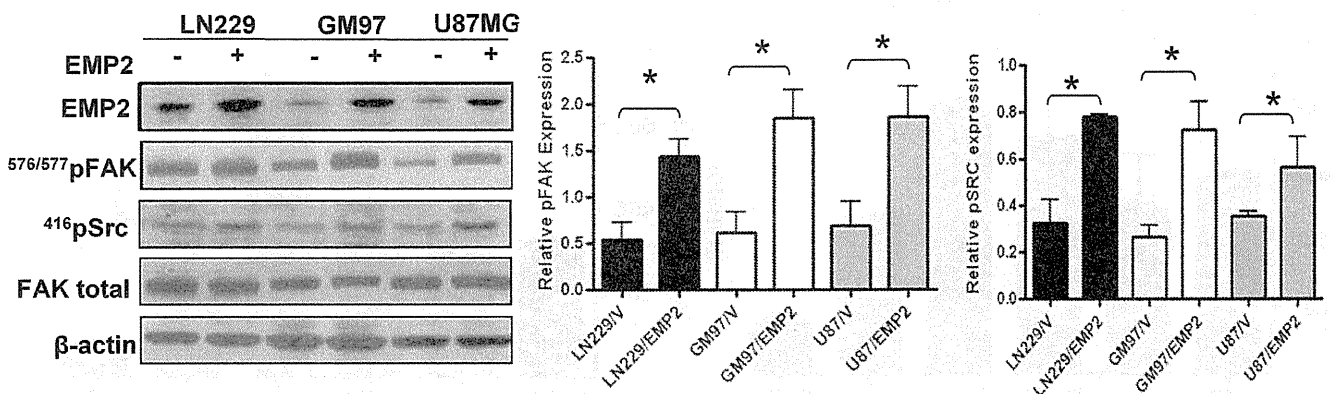




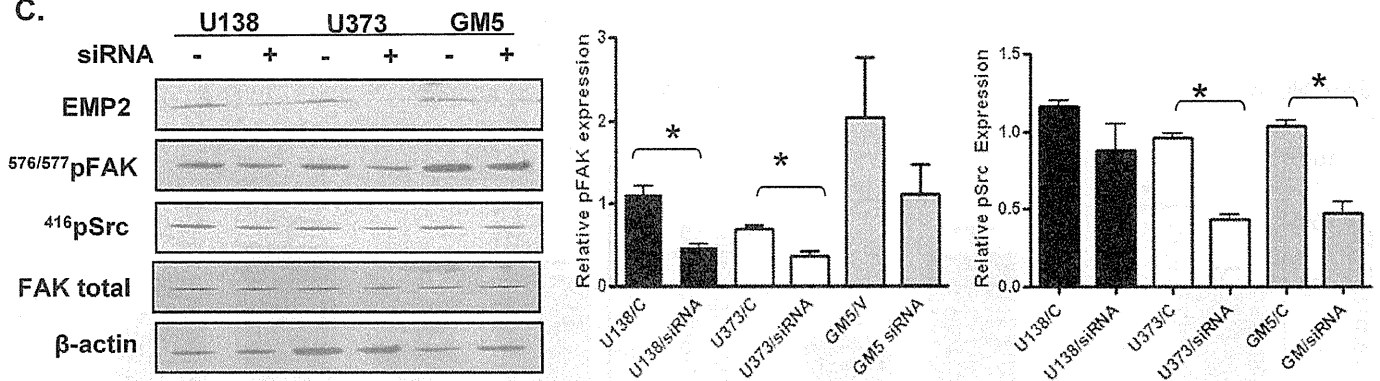
A.



B.



C.





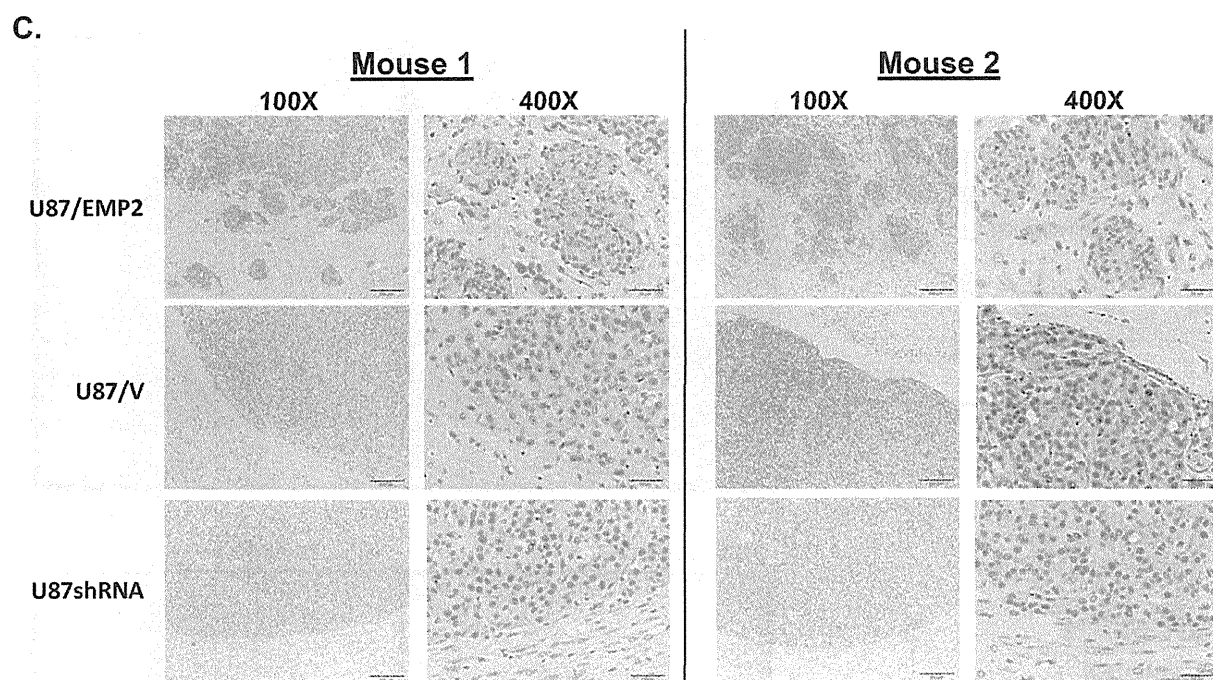
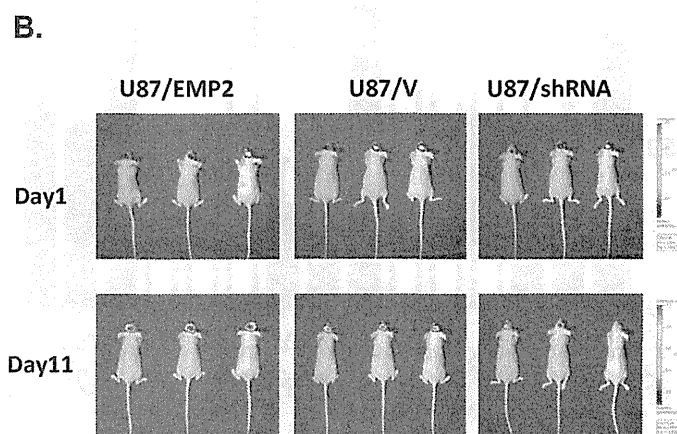
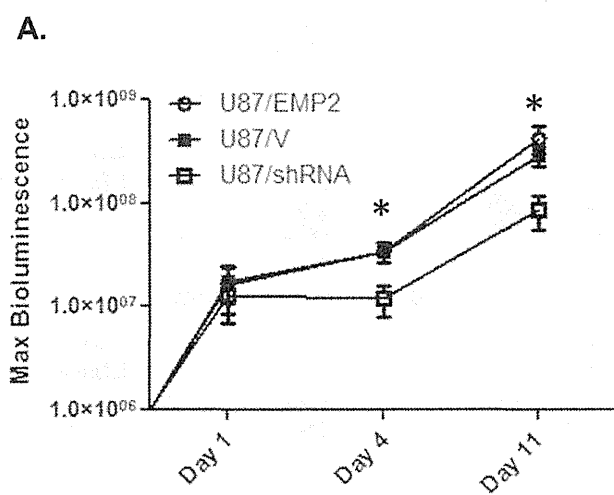


Figure 6

B.

